Hot working of platinum group metal-modified Ni-base superalloys for thermal protection system applications

D.L. Ballard [a,*], D.S. Weaver [a], A.L. Pilchak [b], S.L. Semiatin [a]

[a] *Materials and Manufacturing Directorate, Air Force Research Laboratory, Wright-Patterson Air Force Base, AFRL/RXLM, 2230 10th Street, OH 45433-7817, USA*
[b] *Universal Technology Corporation, 1270 N. Fairfield Road, Dayton, OH 45432, USA*

Abstract

Platinum group metal-modified nickel-base superalloys are being investigated for use in thin gage applications, such as thermal protection systems, due to their strength and inherent oxidation resistance at temperatures in excess of 1000 °C. This paper summarizes deformation behavior and microstructure evolution during multi-hit hot forging and subsequent hot rolling of an experimental two phase γ-Ni + γ'-Ni$_3$Al alloy with a composition of Ni–15Al–5Cr–3Pt–2Ir–0.3Hf (atomic %) with C, B, and Zr additions for grain-boundary refinement and strengthening. The feasibility of hot rolling this material to a final thickness of 250 μm and obtaining a nearly fully recrystallized microstructure was demonstrated. However, an anomalous grain-growth behavior was also observed at the surface in the intermediate and final rolled product.
Published by Elsevier Ltd.

Keywords: Structural application; Grain growth; Superalloy; Thermomechanical processing; Thermal protection systems

1. Introduction

Nickel-base alloys with densities exceeding 8 g/cm^2 may not initially be thought of as viable materials for acreage thermal protection systems (TPS). Indeed, the Space Shuttle utilizes many types of *non-metallic* TPS materials, in both tile and fabric form as well as reinforced carbon–carbon on the nose and wing leading edges.[1] However, shuttle refurbishment between flights has been reported to require >17,000 h of labor,[2] or a level of maintenance which is unacceptable for Air Force applications. Hence, thin gage *metallic* sheet and foil may become an option for TPS because the turn-around time for inspection can be significantly reduced, durability is improved, and replacement time is short because metallic TPS (MTPS) panels are mechanically attached. Indeed honeycomb MTPS was evaluated (Fig. 1) and would have comprised a significant portion of the acreage TPS on the lower surface of the NASA X-33 vehicle,[2] a wedged-shaped subscale prototype of a reusable launch vehicle[3] designed by Lockheed Martin. Nevertheless, while MTPS can play a role in these systems, there will always be a need for non-metallic materials in areas for which an extreme environment (in terms of temperature, stress, etc.) demands properties exceeding those of MTPS.

One experimental class of alloys being evaluated for MTPS applications is platinum group metal (PGM)-modified Ni-base superalloys. Such materials must be capable of being processed to thin gages on the order of 0.25 mm, which is a typical face sheet thickness for metallic honeycomb panels. Platinum-modified nickel aluminide (β-NiAl) compositions, e.g. Ni–50Al–15Pt, are currently used throughout the turbine-engine industry for airfoil coatings because of their oxidation resistance.[4–7] Unfortunately, these compositions are brittle and are not practical for a monolithic application across the service temperature range, particularly below 600 °C.[8,9] On the other hand, research on PGM-modified Ni + Ni$_3$Al ($\gamma + \gamma'$) compositions for bond coats[6,10–11] has suggested that they may be good candidates with regard to environmental resistance due to the formation of an adherent, protective α-alumina scale.[12] In particular, in the late 1970s and early 1980s, Corti et al.[13–15] reported results on the environmental protection associated with various PGM additions to nickel-base superalloys and concluded that platinum had the best overall performance in both oxidizing and sulfidizing environments. Platinum also provided the best strength at temperatures in excess of 1000 °C because it partitions to and strengthens the γ' precipitate phase.[16,17] A high volume fraction of the γ' precipitate phase is desirable for good

---

* Corresponding author. Tel.: +1 937 255 4003; fax: +1 937 255 0445.
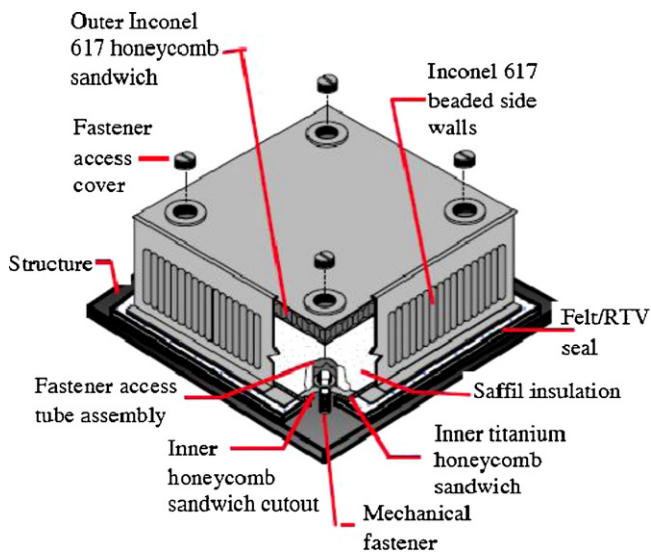*E-mail address:* donna.ballard@wpafb.af.mil (D.L. Ballard).

Fig. 1. One of the proposed X-33 metallic thermal protection system options.

Table 1
Aim versus actual composition of project alloy (atomic percent).

Heat number	Ni	Cr	Al	Hf	C	B	Zr	Pt	Ir
5C (Aim)	74.37	5.00	15.00	0.30	0.25	0.04	0.04	3.00	2.00
5C (Actual)	74.70	4.96	14.84	0.30	0.27	0.06	0.04	2.92	1.92

isostatic pressing (HIP) to seal casting porosity and alloy homogenization. $T_{\gamma'}$ was found to be between 1200 and 1225 °C. The cast bar was thus HIPed using a pressure of 207 MPa at 1250 °C for 8 h. A homogenization heat treatment at 1250 °C for 42 h in air followed by water quenching was then performed. The HIP and homogenization treatments resulted in a γ-Ni matrix with an equiaxed grain size between 1 and 2 mm and sub-micron-size cooling γ'. Fig. 2a shows the as-cast microstructure, while Fig. 2b shows the microstructure following the HIP and homogenization heat treatment.

2.2. Hot compression testing

Two cylinders, each measuring 38-mm length × 25-mm diameter were cut from the HIPed-and-homogenized bar and prepared for isothermal, constant true strain rate hot compression testing at a *supersolvus* temperature to simulate the breakdown process for a coarse-grain microstructure. Specifically, two series of four-hit compression tests were conducted on each cylinder at 1225 °C, 10^{-2} s^{-1} utilizing a 60 s dwell between each hit. The strain increments were 0.2, a level typical of production cogging operations, resulting in a total imposed strain of 1.6. Following compression, the resultant microstructure was examined using back scatter electron imaging (BSEI) on as-polished cross-sections using a Leica Cambridge Stereoscan 360 Field Emission (FE) or a Quanta 600 environmental scanning electron microscope (ESEM).

2.3. Pack rolling

A rectangular preform was cut from each of the two forged pancakes, canned, and hot pack rolled to establish the feasibility of producing wrought sheet and foil via *subsolvus* thermomechanical processing. To this end, samples measuring ∼31 mm × 32 mm × 8.7 mm, were cut by electric-discharge machining (EDM) and belt ground to remove surface imperfections. The rolling cans were fabricated from Waspaloy or alloy 718Plus^{TM}.

Hot pack rolling was performed on a two-high Farrel laboratory mill. In each case, the canned sample (pack) was preheated at 925 °C for 20 min to allow the preform and can temperatures to equilibrate. The pack was then transferred to a furnace at 1190 °C and soaked for 30 min. The reduction per pass was 12%, rolling speed was 7.6 surface m/min, and the pack reheat time between each pass was ∼2.5–3 min. Following the last pass, the pack was slow cooled in vermiculite to minimize thermal stress due to rapid cooling.

The first preform was canned in Waspaloy and unidirectionally rolled to a total reduction of ∼60% yielding a sheet measuring 63 mm × 31.5 mm × 3.6 mm. This

high-temperature strength and adequate creep resistance, which are important design considerations. Iridium is added to the alloy because it partitions almost equally to both γ and γ' – there is a slight preference for the γ phase – and it reduces the lattice mismatch of the alloy.[16,17]

In view of the excellent oxidation resistance of PGM-modified Ni-base superalloys at temperatures in excess of 1000 °C, the associated relatively high material cost may be justified if useful product forms such as thin gage sheet and foil can be readily made by conventional hot working processes. However, processing of superalloys, let alone PGM-modified superalloys into the desired thin gages can be challenging. At present, most of the experience with PGM-modified Ni-base superalloys has been in the area of casting; relatively little has been reported on wrought processing.[18,19] The objective of the present research was to evaluate the hot working characteristics of an experimental PGM-modified Ni-base superalloy and to establish the feasibility of near-conventional processes for producing sheet and foil products of this experimental alloy.

2. Experimental procedures

2.1. Materials

Six 150 g buttons, each with an aim chemistry of Ni–15Al–5Cr–3Pt–2Ir–0.3Hf–0.25C–0.04B–0.04Zr (denoted as 5C), were vacuum arc-melted in the Materials Processing Laboratory at the Materials and Manufacturing Directorate of the Air Force Research Laboratory. The arc-melted buttons were remelted three times to ensure a homogeneous distribution of the alloying elements. Subsequently, the buttons were melted and drop-cast into 25-mm diameter, water-cooled copper molds at the DOE Ames Laboratory in Ames, Iowa. Chemical analysis was performed on the 900 g as-received bar to determine the actual alloy composition (Table 1).

Heat treatments were conducted to determine the γ' solvus temperature ($T_{\gamma'}$) and to establish suitable temperatures for hot
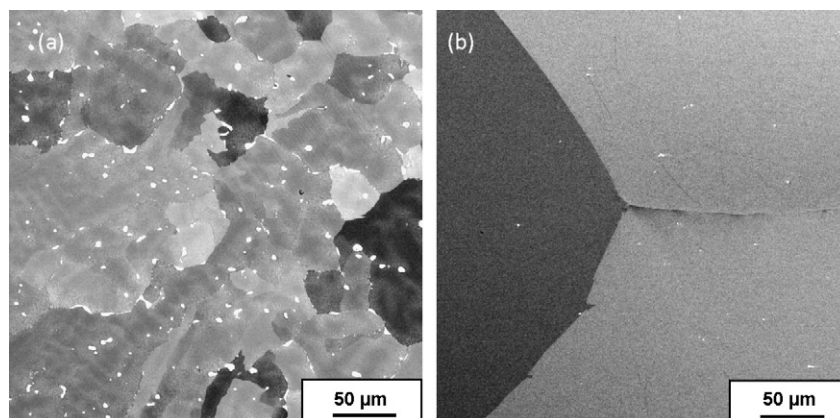
Fig. 2. Microstructures of PGM-modified superalloy: (a) as-received and (b) after solution heat treatment at 1250 °C for 50 h and water quenching.

sheet was trimmed and belt ground (to obtain a piece measuring 63 mm × 31.5 mm × 3.4 mm), recanned in Waspaloy, and unidirectionally rolled again to dimensions of 179 mm × 37 mm × 1.1 mm. After decanning, the sheet was creep flattened in air at 1163 °C for 1 h. Last, a piece measuring 32 mm × 37 mm × 1 mm was EDMed from the sheet, recanned in alloy 718Plus^{TM}, and unidirectionally rolled to foil with dimensions of 127 mm × 38 mm × 0.25 mm. The foil was creep flattened in air at 732 °C for 8 h, followed by forced-convection cooling. The static recrystallization and grain-growth behavior of the foil was determined by conducting heat treatments at 1190 °C for 0.25, 1, 16, and 24 h.

The preform extracted from the second forged pancake was processed to sheet/foil in a similar fashion except that it was reduced to a final thickness of 0.18 mm via perfect cross-rolling in two campaigns, re-canning at an intermediate thickness of 1 mm. The purpose of this alternate processing operation was to determine whether cross-rolling would result in a higher degree of recrystallization or a different grain structure from the unidirectionally rolled preform.

The microstructures developed in as-rolled and rolled-and-recrystallization-heat-treated samples were determined using both BSEI and electron backscatter diffraction (EBSD). EBSD data were acquired in either an FEI Quanta 200 or a Philips/FEI XL-30 ESEM which had tungsten filament and field-emission sources, respectively. EBSD scans were made using step sizes between 0.35 and 3 μm, the exact value depending on the scale of the features of interest in the specimens. Areas between 2 and 10 mm^2 were analyzed using a combination of beam scans and automated stage movement. Limited wavelength dispersive spectroscopy (WDS) scans were conducted on 1-mm thick specimens in either the as-rolled condition or following a 24 h recrystallization heat treatment using a Cameca SX 100 Electron Probe Microanalyzer.

3. Results and discussion

The results of this investigation comprised the (1) stress–strain curves and microstructures from the hot forging experiments and (2) microstructure and texture analysis for the pack-rolled samples. These results were compared to related

observations for a conventional wrought γ + γ′ superalloy ingot material, i.e., Waspaloy.

3.1. Hot forging behavior

Typical flow curves from the multi-hit *supersolvus* hot compression tests on two different samples are shown in Fig. 3. The plastic-flow response during each strain increment was characterized by a very short and steep initial strain-hardening transient followed by a peak stress and negligible subsequent flow softening. Furthermore, the flow stress on reloading following each 60s-dwell tended to be lower than that at the end
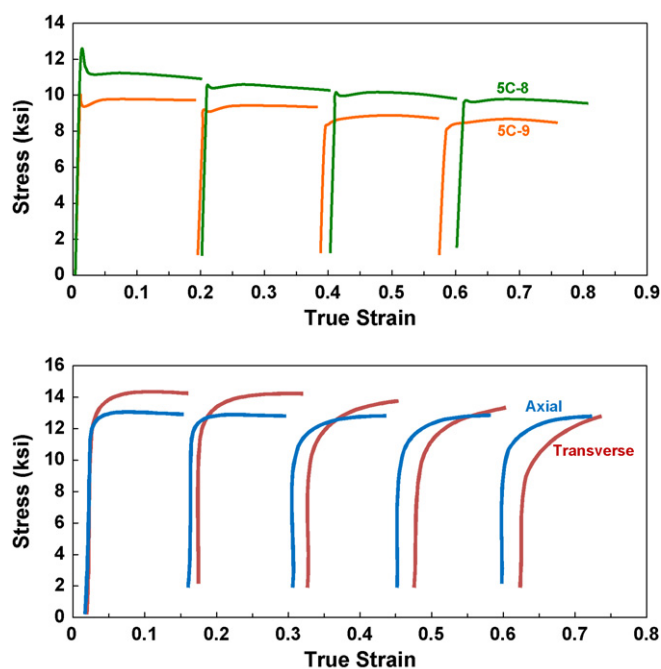

Fig. 3. True stress–true strain curves from multi-hit hot compression tests on: (a) the present PGM-modified superalloy and (b) Waspaloy ingot material. The results in (a) pertain to the second of two series of tests (on two separate samples at 1225 °C, a constant true strain rate of 10^{-2} s^{-1}, using a strain increment of 0.2 and 60 s dwell between hits, resulting in a final overall strain of 1.6. The results in (b) pertain to deformation at 1177 °C, 10^{-1} s^{-1} using five strain increments of 0.15 and 60 s dwell between hits, leading to a total strain of 0.75.
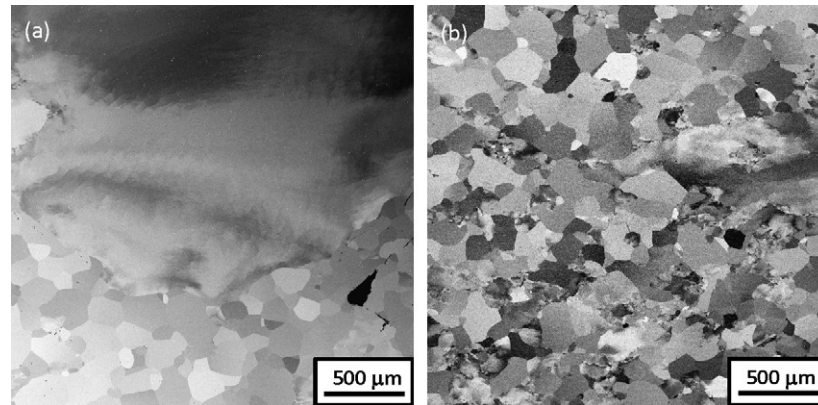
Fig. 4. Observations of the degree of recrystallization in the PGM-modified superalloy following the (a) first and (b) second series of multi-hit hot forging trials.

of the previous increment of deformation. These observations suggested minimal dynamic recrystallization and that a process associated with static softening during the dwell periods was dominant with regard to microstructure evolution.

Microstructure observations suggested that the static softening between hits (as noted in the flow curves) was a result of metadynamic or static recrystallization. In particular, partial recrystallization was observed after the first and second series of hits (Fig. 4). The recrystallized grain size following each series were 100 and 200 μm, a value representing a refinement in grain size of approximately one order of magnitude relative to that for the cast-and-homogenized microstructure.

The deformation and recrystallization behaviors of the PGM-modified superalloy 5C were interpreted in the context of previous observations for supersolvus processing of a conventional $\gamma - \gamma'$ alloy Waspaloy, in ingot form.[20] There were qualitative similarities, but also some important quantitative differences in both test approach and observations. For example, the Waspaloy material was tested at a higher temperature relative to its γ' solvus than 5C ($\sim$140 °C versus $\sim$30 °C), although at a comparable actual temperature (1177 °C for Waspaloy and 1225 °C for 5C) and at a higher strain rate (0.1 s^{-1} versus 0.01 s^{-1}). Nevertheless, the multi-hit stress–strain curves of 5C and Waspaloy (Fig. 3) showed limited or no flow softening during each relatively small imposed strain increment and measurable softening between strain increments, most likely due to metadynamic- and static recrystallization, as mentioned above. In addition, despite the differences in test temperature and strain rate, the flow stresses for Waspaloy and 5C were similar in magnitude. However, when interpreted in the context of the temperature corrected strain rate Z ($Z = \dot{\varepsilon} \exp(Q/RT)$, in which $\dot{\varepsilon}$, Q, R, and T denote strain rate, an apparent activation energy, the gas constant, and absolute temperature), it was concluded that the PGM additions in 5C result in substantially higher flow stress than in Waspaloy for a given Z. In other words, to obtain a flow stress for 5C which is comparable to that for Waspaloy, a lower strain rate and/or a higher temperature is required.

The recrystallization kinetics during multi-hit deformation of 5C were also found to be qualitatively similar to those for Waspaloy ingot material, despite the difference in test temperature (Fig. 5). For Waspaloy ingot with a marked columnar grain structure and associated crystallographic fiber texture, the

recrystallization kinetics were dependent on test orientation.[20,21] Deformation parallel to the columnar grain/fiber texture direction (designated as axial tests, or simply "Ax") exhibited the slowest kinetics, whereas transverse tests (designated as "T") led to more rapid recrystallization. The comparison in Fig. 5 shows that 5C recrystallized approximately the same amount ($\sim$50%) as the axially oriented Waspaloy at low strains ($\sim$0.8). At high strains ($\sim$1.6), Waspaloy tested in either orientation was fully recrystallized and 5C was 90% recrystallized.

The apparent similarities in Fig. 5 can be interpreted in the context of microstructure and solute effects on recrystallization. For Waspaloy, the decrease in recrystallization rate typically associated with a coarse-grain size (and a decreased density of grain-boundary sites for nucleation) was mitigated by additional nucleation sites at carbide particles; i.e., particle-stimulated nucleation (PSN) of recrystallization. On the other hand, the PGM-modified Ni-base superalloy had a much smaller (and equiaxed) starting grain size in comparison with the Waspaloy ingot, which in and of itself would tend to produce more rapid recrystallization kinetics. Furthermore, it was deformed at a higher temperature, which would tend to increase grain-boundary mobility. The observed retardation in kinetics relative
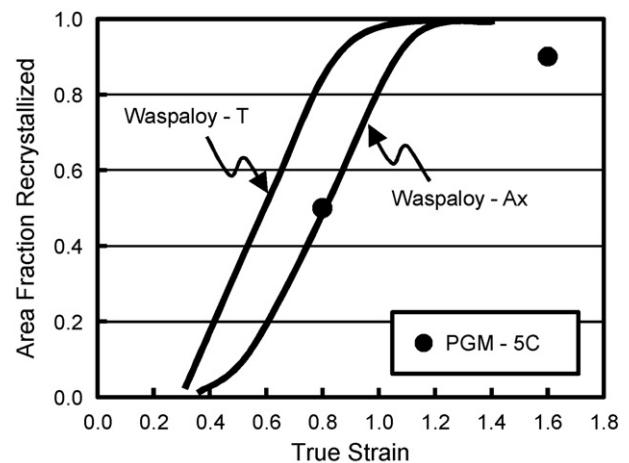

Fig. 5. Comparison of measurements of the recrystallized fraction as a function of strain for supersolvus multi-hit forging of cast-and-homogenized PGM-modified superalloy and Waspaloy.
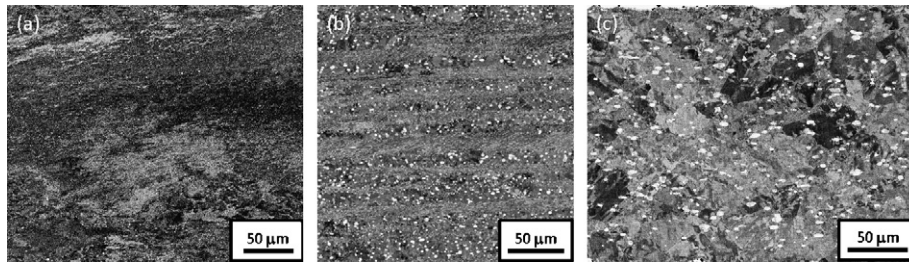
Fig. 6. BSEI microstructures following total thickness reductions (in %) of (a) 60, (b) 87, and (c) 97. The rolling direction is horizontal, and the sheet normal direction is vertical in all micrographs.

to those for Waspaloy ingot must therefore be associated with two effects, the absence of PSN (due to the limited number of coarse carbides in 5C) and the drag exerted by PGM solute elements on migrating grain boundaries. The former effect might be reduced in a large PGM-modified Ni-base superalloy ingot if coarse carbides can be produced. However, the solute drag effect would not be affected. Based on the present observations, it is thus hypothesized that commercial-scale PGM superalloy ingots may be somewhat more difficult to breakdown than ingots of conventional superalloys such as Waspaloy.

3.2. Hot rolling behavior

Visual observations of rolled and decanned pieces revealed that the experimental PGM-modified Ni-base superalloy material can be successfully hot pack rolled at temperatures approximately 15–25 °C below the γ' solvus temperature. Using a novel can design, sheet and foil of relatively uniform gage and without surface and edge cracks were produced. Preform thickness uniformity was found to affect the flatness of finished sheet and foil, however. The variation in initial preform thickness was rather low (0.05 and 0.03 mm), and represented a small fraction of the overall thickness for the first two campaigns of unidirectional rolling; relatively flat pieces were obtained in these campaigns. By contrast, the initial thickness variation was 0.2 mm for the third unidirectional rolling campaign and is believed to have led to a lack of flatness following rolling and creep flattening.

3.3. BSEI observations

BSEI observations elucidated the microstructures developed during the three successive unidirectional rolling campaigns (Fig. 6). The SEM micrographs revealed a large fraction of recrystallized grains which were much finer than those resulting from the supersolvus breakdown. The refined microstructure can be attributed to the pinning effect of second-phase γ' particles.[22] Unrecrystallized bands parallel to the rolling direction were also observed. The number and size of the unrecrystallized bands decreased with increasing reduction/strain (Fig. 6). The cross-rolled specimen, deformed to the same reduction as the unidirectionally rolled sample, showed similar unrecrystallized bands.

An unusual grain-growth phenomenon was also observed at the surface during the final heat treatment of the unidirectionally

rolled sheet as well as at the surface of the as-rolled specimen itself.[23] In particular, a band of columnar-like grains (i.e., those whose boundaries were normal to the surface) appeared to grow from the surface. To a first order, the depth of these grains, d, appeared to follow an approximately parabolic dependence on heat-treatment time, $d \sim t^{0.5}$ (Fig. 7). The source of the anomalous surface grain structure was determined to be most likely chemical in nature. Specifically, WDS indicated that aluminum was lost during heat treatment. The composition of the as-rolled sheet was Ni–14.6Al–5.2Cr–0.3Hf–3Pt–2Ir + C, B, Zr. By contrast, the composition of the large grains at the surface was Ni–12.7Al–5.1Cr–0.2Hf–3.1Pt–2.1Ir + C, B, Zr following the 24 h heat treatment. The surface also appeared to consist of a zone denuded of γ' particles. The coarsened center of the sheet was also somewhat depleted of aluminum; its composition was Ni–13.9Al–5.2Cr–0.3Hf–3Pt–2.1Ir + C, B, Zr, but there were still γ' particles present here. The 1100 °C isotherm for the ternary Ni–Al–Pt phase diagram[7] confirms that lowering the effective aluminum concentration quickly places one in the single-phase γ region. The observed depletion is a result of outward diffusion of aluminum to form an alumina scale. While this scale is desirable, it can be a disadvantage when the depletion results in a loss of the pinning particles. The alloy does contain carbon and boron which should play a role in grain-boundary pinning; however, the observations do not support a large enough
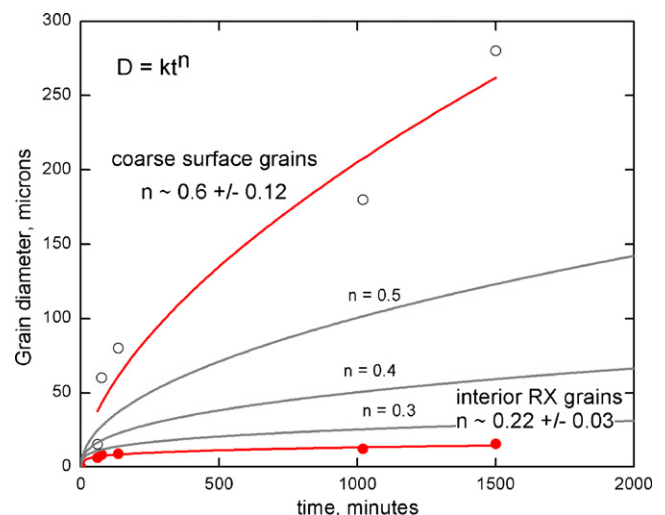

Fig. 7. Measured grain-growth kinetics for interior recrystallized grains and coarse surface grains.
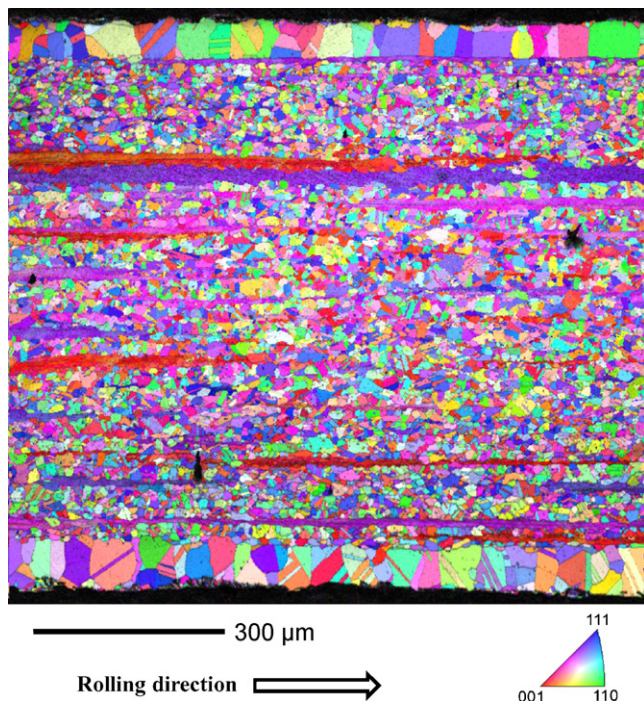
Fig. 8. Rolling direction inverse-pole-figure map of the PGM-modified super-alloy sheet after unidirectional rolling and recrystallization heat treatment at 1190 °C for 15 min. The rolling direction is horizontal and the sheet normal direction is vertical.

volume fraction of either carbides or borides to affect pinning of the surface grains. On the other hand, the rather slow growth of the *equiaxed* grains at the center of the sheet (i.e., $d \sim t^{0.2}$, Fig. 7) does suggest a substantial Zener drag due to γ' precipitates here. These phenomena are now being investigated in more detail.

The unusual grain-growth phenomenon was also observed, but to a lesser degree, in the cross-rolled sheet, a trend that might be attributed to the shorter high-temperature static exposure of this sheet associated with reduced heating, reheating, and flattening times.

3.4. EBSD observations

Specimens were examined using electron backscatter diffraction (EBSD) in the as-rolled and flattened condition, as well as after recrystallization heat treatment at 1190 °C for 15 min, 1, 16 and 24 h.

A representative EBSD scan from the specimen heat treated for 15 min is shown in Fig. 8. This image reveals the three characteristic features observed in both the as-rolled and rolled-and-recrystallized conditions, namely, elongated bands, fine recrystallized grains and coarse recrystallized grains on the surfaces of the sample. Thus, this image serves as a useful basis for qualitatively discussing microstructural evolution during rolling and post-rolling heat treatment.

After the 15 min heat treatment at the rolling temperature (1190 °C), approximately 20% of the material was unrecrystallized, and the microstructure included high aspect ratio features that were often several millimeters long, but generally 30–50 μm thick. When viewed from the rolling plane, the unrecrystallized

regions were typically between 200 and 500 μm in the transverse direction. Outside the unrecrystallized regions, there were areas of similar thickness that contained fine, recrystallized grains with an average diameter of 6 μm. These recrystallized grains often contained a significant fraction of $\Sigma 3$ twin boundaries; no twins were observed within the unrecrystallized regions, e.g. there was no deformation twinning.

Semiatin et al.[21] and Weaver and Semiatin[20] have shown that the recrystallization and grain-growth kinetics of Waspaloy during breakdown of the initial ingot structure may exhibit a strong orientation dependence. Thus, it is likely that some of the initial grains were not recrystallized during the primary forging of the cast-and-homogenized material and were present in the rolling preform during subsequent rolling. During the rolling operations, these grains could have been elongated in the rolling direction and, depending on their initial orientation with respect to the plane-strain deformation imposed during rolling, were either recrystallized or evolved into one of the elongated bands such as those shown in Fig. 8. These banded regions generally contained networks of low angle boundaries ($\leq 15°$), although the orientation gradients were continuous such that the local point-to-point misorientation was typically less than 2°.

Some of the unrecrystallized bands maintained nearly constant orientation along their length while others contained significant orientation gradients, with lattice rotations as large as 60° measured in some cases. The unrecrystallized regions were found to be primarily in orientations that were stable with respect to the plane-strain compression deformation imposed by rolling.[24] The most frequently observed bands were those with the brass {1 1 0} <1 1 2> and S1 {1 2 4} <1 1 2> orientations although copper {1 1 2} <1 1 1>, Goss {1 1 0} <0 0 1>, S3 {1 2 3} <6 3 4> and Taylor {4 4 11} <11 11 8> bands were also observed less frequently. Unrecrystallized cube {0 0 1} <1 0 0> oriented bands were also identified which are not considered to be in an ideal, or stable, orientation. The fraction of cube bands in the microstructure was slightly higher than the fraction of brass oriented bands. Ridha and Hutchinson[25] have suggested that cube-oriented bands are persistent during rolling because they have lower-than-average stored energy. These authors have suggested this is a consequence of the fact that active slip systems in cube-oriented bands have orthogonal Burgers vectors which cannot interact elastically. Using TEM, Samajdar and Doherty[26] have also observed lower dislocation densities consistent with a smaller degree of stored work in cube-oriented bands.

With increasing time at the recrystallization temperature, the unrecrystallized bands described above were consumed as adjacent recrystallization fronts swept through them, or new grains nucleated within the bands and grew outward. Due to the lower amount of stored energy within the bands, the former mechanism was observed much more frequently. The elongated unrecrystallized bands were observed in the as-rolled and flattened conditions as well as in the 15 min and 1 h heat treated samples. However, they were completely consumed during the 16 h anneal by the fine equiaxed grains which were undergoing simultaneous growth themselves. The S oriented bands were consumed first during heat treatment with the fraction of bands reducing by two-thirds after only 15 min at 1190 °C. This is con-
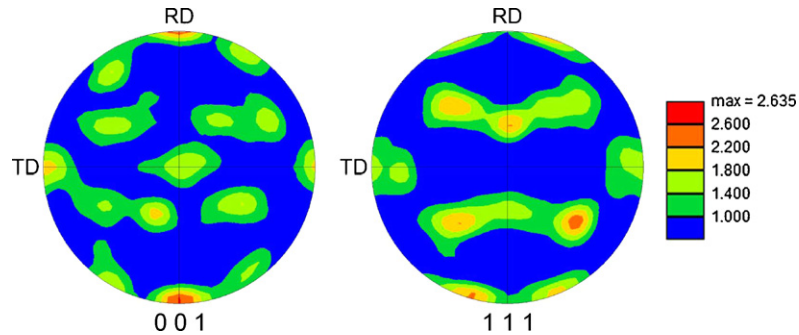
Fig. 9. Pole figures for the unidirectionally rolled sheet after heat treatment at 1190 °C for 1 h.

sistent with the observations of Samajdar and Doherty[26] who reported that S orientations generally have higher stored energy and thus recrystallize readily. In general, bands in the cube orientation were the most resistant to recrystallization and persisted the longest during heat treatment; this is consistent with cube grains having a low Taylor factor and thus a relatively small amount of stored work. The brass orientation {1 1 0} <1 1 2> appeared to be the second most resistant to recrystallization.

As the bands were consumed by the fine recrystallized grains, a change in texture was observed. In the as-rolled and flattened condition, the large size and moderately high volume fraction of bands (~40%) gave them substantial weight in the orientation distribution function and so the texture was dominated by these components. After heat treatment, once the bands were consumed, the texture was dominated by the fine recrystallized grains. The intensities of the deformation and recrystallization texture components were as high as 8 for short heat treatment times (15 min) and dropped to 5 at long times (24 h) consistent with a moderate strength texture within the sheet.

At short times, when the texture transition is only partially complete, both types of texture components can be readily identified in pole figures. An example is shown in Fig. 9 which shows the texture of the sheet after 15 min at 1190 °C.[24] The cube texture is evident as intensities at RD, TD and ND in the 0 0 1 pole figure. In addition to the cube-oriented grains, there were additional grains which had <0 0 1> || rolling direction as evidenced by the higher intensity poles at RD compared to either TD or ND. It is also noteworthy that there were many Σ3 twins observed within the fine recrystallized grains between the bands, which gave rise to the twin of the cube recrystallization texture. This is typical of rolled-and-recrystallized FCC metals.[24] EBSD also revealed that almost all of the unusual coarse, columnar-like grains at the surface of the unidirectionally rolled sheet, whose extent increased during heat treatment, contained Σ3 twins. The growth front remained planar regardless of whether the columnar grains bordered fine, equiaxed, recrystallized grains or coarse, elongated unrecrystallized bands. It may thus be hypothesized that grain-boundary migration was not strongly dependent on local misorientation. Furthermore, the grains did not exhibit any preferred orientation implying that they were not the product of an oriented nucleation or preferred-growth mechanism.

4. Summary and conclusions

Using near-conventional forging and pack-rolling practices in terms of temperatures and strain rates, an experimental cast-and-homogenized PGM-modified nickel-base superalloy was successfully broken down and rolled to foil having a thickness (~200 μm) approaching that for MTPS face sheet material. Although multiple thermomechanical processing steps were required, nearly fully recrystallized microstructures with a grain size of ~150 or ~8 μm were achieved following supersolvus breakdown and subsolvus hot rolling, respectively.

The supersolvus recrystallization behavior was qualitatively similar to that of Waspaloy. In addition, EBSD analysis provided insight into microstructure and texture evolution during subsolvus hot rolling and subsequent heat treatment. In particular, unrecrystallized bands having textures close to the ideal orientations associated with plane-strain compression of FCC metals were observed in as-rolled sheet. During heat treatment, the deformed bands were consumed as the adjacent fine grains grew into them. Unrecrystallized grains in the cube and brass orientations persisted the longest during heat treatment. In addition, a region of coarse recrystallized grains was developed at the free surfaces of 1-mm sheet product and grew toward the center during annealing. These grains typically contained a high fraction of Σ3 boundaries, but did not show any tendency for oriented nucleation or preferred growth.

It is believed that upon gaining a better understanding of the effects of processing on recrystallization and grain growth, an alloy of similar composition having the benefits of inherent oxidation resistance and elevated temperature strength can be fabricated.

Acknowledgments

References

1. Avallone EA, Baumeister III T, Sadegh AM, editors. *Standard handbook for mechanical engineers*. New York: McGraw-Hill; 2007. p. 11–104–108.
2. Blosser ML. *Development of metallic thermal protection systems for the reusable launch vehicle*. NASA-TM-110296; 1996.
3. Reusable launch vehicle program fact sheet, NASA website, http://www.hq.nasa.gov/office/pao/History/x-33/rlv_facts.htm.
4. Sims CT, Stoloff NS, Hagel WC. *Superalloys II*. New York: John Wiley and Sons; 1987. p. 301–10.
5. Sims CT, Stoloff NS, Hagel WC. *Superalloys II*. New York: John Wiley and Sons; 1987. p. 368–9.
6. Gleeson B, Wang W, Hayashi S, Sordelet DJ. Effects of platinum on the interdiffusion and oxidation behavior of Ni–Al-based alloys. *Mater Sci Forum* 2004;**461-464**:213–22.
7. Hayashi S, Ford SI, Young DJ, Sordelet DJ, Besser MF, Gleeson B. α-NiPt(Al) and phase equilibria in the Ni–Al–Pt system at 1150 °C. *Acta Mater* 2005;**53**:3319–28.
8. Pan D, Chen MW, Wright PK, Hemker KJ. Evolution of a diffusion aluminide bond coat for thermal barrier coatings during thermal cycling. *Acta Mater* 2003;**51**(issue 8):2205–17.
9. Taylor MP, Evans HE, Busso EP, Qian ZQ. Creep properties of a Pt-aluminide coating. *Acta Mater* 2006;**54**(issue 12):3241–52.
10. Izumi T, Gleeson B. Oxidation behavior of Pt + Hf-modified γ-Ni + γ'-Ni$_3$Al alloys. *Mater Sci Forum* 2006;**522/523**:221–8.
11. Hayashi S, Narita T, Gleeson B. Early-stage oxidation behavior of γ'-Ni$_3$Al-based alloys with and without Pt addition. *Mater Sci Forum* 2006;**522-523**:229–38.
12. Tatlock GJ, Hurd TJ, Punni JS. High temperature degradation of nickel-based alloys. *Platinum Metals Rev* 1987;**31**:26–31.
13. Coupland DR, Corti CW, Selman GL. The PGM concept: enhanced corrosion resistant superalloys for industrial and aerospace applications. In: *Proceedings of the Pettern Intl Conf. on the behaviour of high temperature alloys in aggressive environments*. 1979.
14. Corti CW, Coupland DR, Selman GL. Platinum-enriched superalloys-enhanced oxidation and corrosion resistance for industrial and aerospace applications. *Platinum Metals Rev* 1980;**24**:2–11.
15. Coupland DR, Hall CW, McGill IR. Platinum-enriched superalloys-A developmental alloy for use in industrial and marine gas turbine environments. *Platinum Metals Rev* 1982;**26**:146–57.
16. Murakami H, Honma T, Koizumi Y, Harada H. Distribution of platinum group metals in Ni-base single-crystal superalloys. *Superalloys* 2000:747–56.
17. Heidloff AJ, Van Sluytman J, Pollock TM, Gleeson B. Structural stability of platinum-group-metal-modified $\gamma + \gamma'$ Ni-base alloys. *Metall Mater Trans A* 2009;**40A**:1529–40.
18. Borodians'ka H, Demura M, Kishida K, Hirano T. Fabrication of thin foils of binary Ni-Al γ/γ' two-phase alloys by cold rolling. *Intermetallics* 2002;**10**:255–62.
19. Chang H, Baker I. Isothermal annealing of cold-rolled high-purity nickel. *Mater Sci Eng A* 2008;**476**:46–59.
20. Weaver DS, Semiatin SL. Recrystallization and grain-growth behavior of a nickel-base superalloy during multi-hit deformation. *Scr Mater* 2007;**57**:1044–7.
21. Semiatin SL, Weaver DS, Fagin PN, Glavicic MG, Goetz RL, Frey ND, Kramb RC, Antony MM. Deformation and recrystallization behavior during hot working of a coarse-grain, nickel-base superalloy ingot material. *Metall Mater Trans A* 2004;**35A**:679–93.
22. Buschow KHJ, Cahn RW, Flemings MC, Ilschner B, Kramer EJ, Mahajan S. *Zener pinning, encyclopedia of materials: science and technology* 2008;**1–11**:9855–9.
23. Buschow KHJ, Cahn RW, Flemings MC, Ilschner B, Kramer EJ, Mahajan S. *Abnormal grain growth, encyclopedia of materials: science and technology* 2008;**1–11**:3634–6.
24. Kocks UF, Tome CN, Wenk HR. *Texture and anisotropy: preferred orientations in polycrystals and their effect on materials properties*. Cambridge, UK: Cambridge University Press; 1998.
25. Ridha AA, Hutchinson WB. Recrystallization mechanisms and the origin of cube texture in copper. *Acta Metall* 1982;**30**:1929–39.
26. Samajdar I, Doherty RD. Cube recrystallization texture in warm deformed aluminum: understanding and prediction. *Acta Mater* 1998;**46**:3145–58.